ISSN: 2319-8753

International Journal of Innovative Research in Science, Engineering and Technology

(An ISO 3297: 2007 Certified Organization)

Vol. 3, Issue 9, September 2014

FTIR and Thermal Studies of Gel Grown Lead Cobalt Mixed Levo Tartrate Crystals

Harshkant Jethva[1*], Mihir Joshi[1]

Ph. D. Student, Department of Physics, Saurashtra University, Rajkot, Gujarat, India[1*]

Professor, Department of Physics, Saurashtra University, Rajkot, Gujarat, India[1]

ABSTRACT: Lead-cobalt mixed levo tartrate crystals for different compositions of lead and cobalt were grown by using single diffusion gel growth method in silica hydro gel medium. Long and dendrite type white crystals as well as spherulitic crystals were obtained. The metallic composition in the crystals was estimated by EDAX. It was found that the metallic composition in the crystals did not vary as per the composition of supernatant solution, i.e., lead content was found more than cobalt content. The powder XRD suggested the orthorhombic nature for all crystals. The grown crystals were characterized by FTIR spectroscopy and thermal studies. The FTIR spectra revealed the presence of water molecules, O-H, C-H, C-O and C=O functional groups. The thermo-grams suggested that the crystals were thermally unstable and decomposed into oxide through carbonate stage.

KEY WORDS: Lead-cobalt mixed levo tartrate crystals, gel growth, FTIR, powder XRD, TG.

I. INTRODUCTION

The gel growth technique is one of the best alternatives for the growth of crystals which are sparingly soluble in water and decompose before melting. Gel acts as a 3-dimensional crucible which supports the growing crystal and at the same time yields to its growth without exerting major forces on it. Growth mechanism of crystal can be directly observed [1]. Nucleation can be controlled by concentration programming and by using dummy gel too [2].

In the literature, many tartrate compounds are reported which have been grown by the gel technique, for example, iron tartrate [3], cobalt tartrate [4-6], lead tartrate [7], mixed iron-manganese tartrate [8] and ternary iron-manganese-cobalt tartrate [9] as well as ternary iron-manganese-nickel tartrate [10]. Carbonate solutions containing Co(II) tartrate complexes find application in an electrochemical procedure of anodic deposition of cobalt oxyhydroxide film on a glassy carbon substrate in an alkali medium [11], whereas, lead tartrate finds application as an additive in gasoline to increase the performance of the engine [12]. This prompted the present authors to grow cobalt and lead mixed levo tartrate crystals by varying the compositions and characterize them by EDAX, Powder XRD, FTIR and TG.

II. MATERIALS AND METHOD

Sodium metasilicate solution of density 1.05 gm/cm^3 was used for preparation of gel. Solution of 1 molar levo tartaric acid was mixed with the solution of sodium metasilicate and the pH of the mixture was kept at 4.5. The mixture was poured in different test tubes of 25 mm diameter and 140 mm length to set into the gel. The supernatant solutions containing different proportions of 1 M lead nitrate and 1 M cobalt nitrate solutions were gently poured on the set gel without disturbing the gel surfaces. The composition of the supernatant was as under.

(I) 1 M, 2 ml $Pb(NO_3)_2$ + 1 M, 8 ml $Co(NO_3)_2{\cdot}6H_2O$
(II) 1 M, 4 ml $Pb(NO_3)_2$ + 1 M, 6 ml $Co(NO_3)_2{\cdot}6H_2O$
(III) 1 M, 6 ml $Pb(NO_3)_2$ + 1 M, 4 ml $Co(NO_3)_2{\cdot}6H_2O$
(IV) 1 M, 8 ml $Pb(NO_3)_2$ + 1 M, 2 ml $Co(NO_3)_2{\cdot}6H_2O$

All the chemicals were AR grade and obtained from Ranbaxy chemicals. The following reaction is expected to occur.

DOI: 10.15680/IJIRSET.2014.0310016

ISSN: 2319-8753

International Journal of Innovative Research in Science, Engineering and Technology

(An ISO 3297: 2007 Certified Organization)

Vol. 3, Issue 9, September 2014

$(1 - X)Pb(NO_3)_2 + XCo(NO_3)_2{\cdot}6H_2O + H_2C_4H_4O_6 + nH_2O \rightarrow Co_XPb_{(1-X)}C_4H_4O_6{\cdot}\ nH_2O + 4HNO_3 + 5H_2O + 1/2O_2$.
Where X = 0.8, 0.6, 0.4and 0.2. Exact value of X is to be determined from EDAX analysis. The amount of HNO_3 produced is very less in comparison to the nutrients being supplied to the growing crystals and hence no major limitation is imposed [7,10,13]. The growth was completed within twenty days. The nature of the grown crystals was dendrite type for all the samples, but the density of the dendrite crystals and their lengths changed as per the composition of the supernatant solutions. Growth of crystals inside the test tubes is shown in figure 1(a), 1(b), 1(c) and 1(d) for the solution (I), (II), (III) and (IV), respectively. In the test tubes the dendrites were found to be originating from the gel-liquid interface. At the bottom of the test tubes some spherulitic type or star type crystals were observed. The coloration of the crystals changed as the composition of the supernatant solution changed.

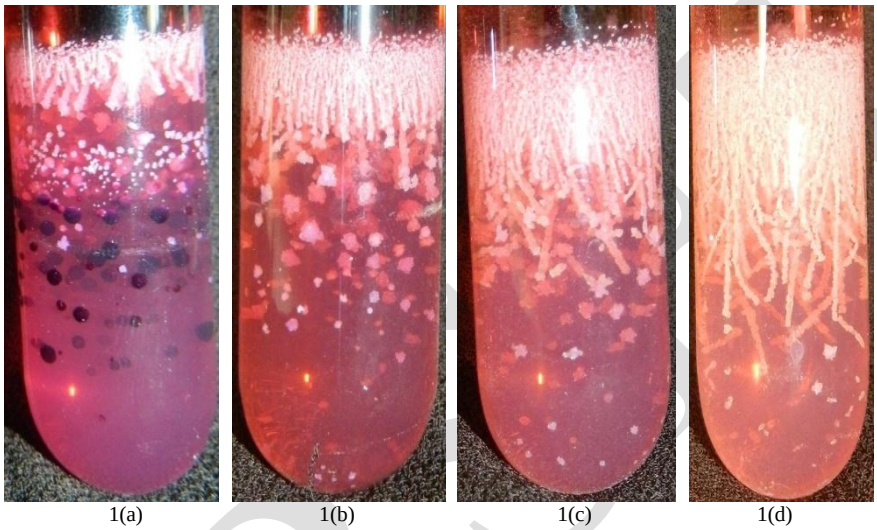

1(a) 1(b) 1(c) 1(d)

Fig. 1. Growth of crystals inside the test tube

III. CHARACTERIZATION TECHNIQUES

The grown crystals were characterized by different techniques. The EDAX was carried out on Philips XL – 30 set up. The Powder XRD patterns were recorded on Philips X'pert MPD by using Cu K_α radiation and the data were analyzed by software powder-x. The FTIR spectra were recorded on Perkin Elmer Spectrum GX spectrophotometer in the range from 400-4000 cm^{-1} in KBr medium. The TG was conducted on Linseis (STA PT 1600) from room temperature to 700^oC at a heating rate of 10^oC/min in atmosphere of air in standard Al_2O_3 crucible.

IV. RESULT AND DISCUSSION

From figure 1 (a-d), one observes that in the test tubes along with dendrite crystals either spherulitic or star type crystals are grown. The composition of grown crystals was determined by EDAX and listed in the table 1 for the crystals grown near the interface of the gel and at the depth of about 3 cm from the gel-liquid interface.

Table 1. EDAX result for Pb Co mixed levo tartrate crystals

Sample No.	Expected atomic weight (%)		Observed atomic weight (%) (From EDAX)			
			crystals near the gel interface		crystals below the gel interface	
	Pb	Co	Pb	Co	Pb	Co
I.	20	80	98.68	1.32	45.79	54.21

DOI: 10.15680/IJIRSET.2014.0310016

ISSN: 2319-8753

International Journal of Innovative Research in Science, Engineering and Technology

(An ISO 3297: 2007 Certified Organization)

Vol. 3, Issue 9, September 2014

II.	40	60	99.39	0.61	99.33	0.67
III.	60	40	99.66	0.34	99.43	0.57
IV.	80	20	99.78	0.22	99.76	0.24

From table 1, it is observed that in the case of sample (II-IV), the percentage weight of Pb is slightly high in the dendrite type crystals at the gel-liquid interface than in the star type or spiky spherulitic crystals at the bottom of the gel. In case of sample (I), the percentage weight of Pb is high in the dendrite crystals at the gel-liquid interface, while percentage weight of Co is high in the spherulitic crystals at the bottom of the gel. There is a clear compositional difference between dendrite type crystals at the gel-liquid interface and spherulitic crystals at the bottom of gel column for the sample (I). There is no significant compositional difference found for the dendrite crystals at the gel-liquid interface and star type crystals at the bottom of gel column for the sample (II-IV). Mechanism of dendrite crystal growth was studied by Fujiwara and Nakajima [14]. Dendrite type growth morphology has been observed by several authors in the gel grown crystals, such as lead tartrate [15], cadmium tartrate [16], ammonium tartrate [17] and lanthanum tartrate [18]. In the present study to grow lead and cobalt mixed levo tartrate crystals, the supernatant ions of Pb^{+2} and Co^{+2} slowly diffused into the gel medium where they react with tartrate anions already present. The crystal growth was started about two days after pouring the supernatant solution at the gel liquid interface in the form of a thin layer of very small crystalline particles. As the content of lead was increased in the supernatant solution, this layer became dense and thick with white crystals in dendrite form, which was due to fast growth rate in one direction and unstable growth front. However, it was observed that as the supernatant reactants percolated through the porous gel, the controlled reaction occurred at the depth of about 3 cm in the gel column, which was almost uniform in all directions and hence spherulitic or spiky spherulitic crystals were grown at the bottom of the test tubes. Earlier Joseph et al [3] explained the growth of spherulitic crystals of iron tartrate in gel medium and also reported the spherulitic growth of iron and cobalt mixed tartarte crystals [19]. The lead tartrate crystals are white and dendrite in form [7] while cobalt tartrate crystals are dark brownish with spherical shape [5]. The proposed and estimated formula for the Pb Co mixed levo tartrate crystals are listed in the table 6.

It is found that as the volume of lead nitrate is increased in the supernatant solution, the wt% of lead entering the lattice is also increased but cobalt does not enter the lattice as per the volume of cobalt nitrate in the supernatant solution. The reason can be explained on the basis of hydrated radii. In the solution, Pb^{+2} and Co^{+2} ions possess a primary hydration shell, which is the number of water molecules directly coordinated to both the metal ions. There is also overall solvation number, which is defined as the total number of water molecules associated when the solvent is water, on which both the ions exercise a substantial restraining influence. Then the successive layers of water molecules are termed as the secondary hydration layers. Hydration of an ion depends on the electrostatic attraction of water molecules to that ion. Attraction of water molecules around an ion depends on the density of charge of ion. The smaller ions having greater ionic potential attract more water molecules. The result is the inverse relationship between non-hydrated radius and hydrated radius. The non-hydrated radius of Pb^{+2} is 1.19 Å and second ionization potential is 15.028 eV while the same quantity for Co^{+2} are 0.65 Å and 17.06 eV, respectively. Therefore, the reverse nature is observed for hydrated radii of Pb^{+2} and Co^{+2} than that for the non-hydrated ones [20,21]. As the hydrated radii of Pb^{+2} being smaller than the hydrated radii of Co^{+2}, the Pb^{+2} ions enter into the reaction in higher concentration than Co^{+2} ions, which is resulting higher concentration of Pb in grown crystals than Co. For the spherulitic crystals below gel-liquid interface for supernatant solution I, the %wt of Co is more than that of Pb. This can be explained on the basis of reactivity. The higher the ionization potential, the more difficult is to remove an electron and hence the less reactive the element is available. In this case, the ionization potential of Co^{+2} ions is more than that of Pb^{+2} ions. Therefore, Co^{+2} ions are less reactive and enter the gel deeper, which results into spherulitic growth of crystals with higher content of Co^{+2} ions. Also, the Pb^{+2} ions being more reactive and their higher concentration is available at the gel-liquid interface, therefore, they are mainly responsible for dendritc crystal growth. But as one moves deeper in to the gel the concentration of Pb^{+2} ions in the gel column decreases as those are used up in the dendritic growth and hence in the spherulitic crystals the concentration of Pb^{+2} ions is comparatively less than that of the dendritic crystals.

It can be noticed from table 1 that except for sample (I), in all samples the weight percent of cobalt is well below 1% and hence only for the sample (I) spherulitic crystals grown in the bottom of gel column are characterized by FTIR, powder XRD and TG.

DOI: 10.15680/IJIRSET.2014.0310016

ISSN: 2319-8753

International Journal of Innovative Research in Science, Engineering and Technology

(An ISO 3297: 2007 Certified Organization)

Vol. 3, Issue 9, September 2014

Powder XRD Study

The powder XRD pattern of the grown crystals at gel-liquid interface for the samples (I-IV) and below gel-liquid interface for sample (I) are shown the figure 2.

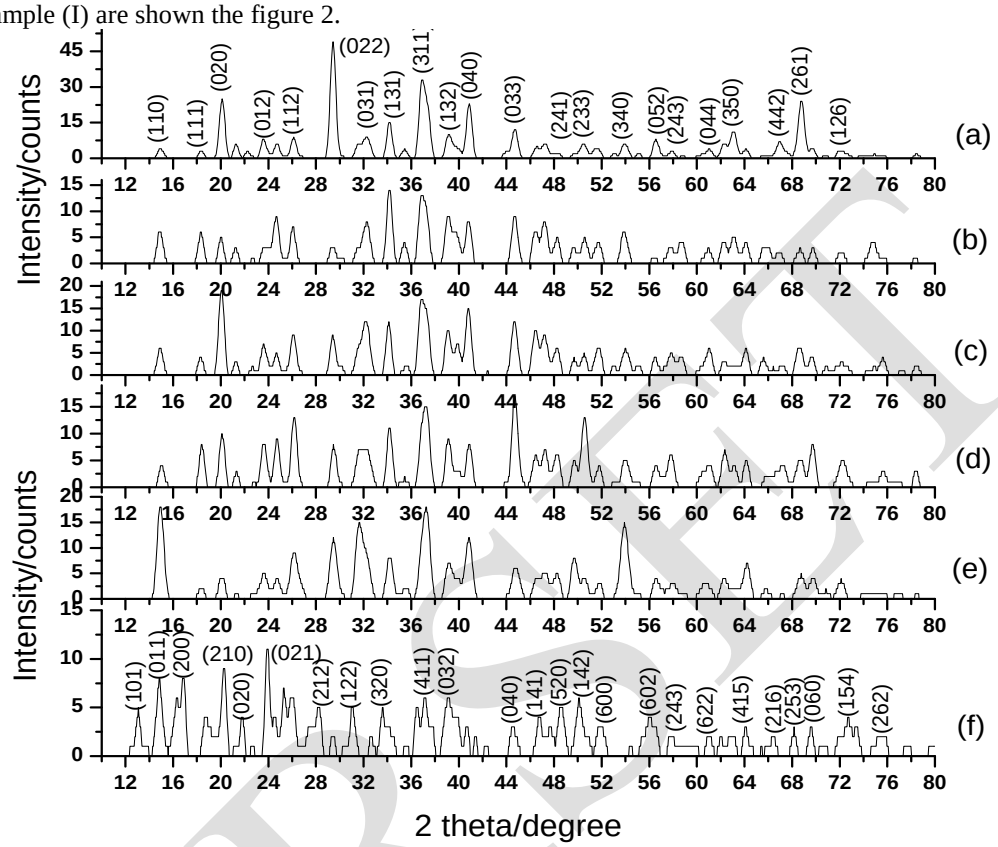

Fig. 2. XRD patterns (a) pure lead tartrate (b) sample I (c) sample II (d) sample III (e) sample IV for dendrite crystals and (f) sample I for spherelutic crystals

The unit cell parameters were computed by using computer software Powder-X and are given in table 2. The orthorhombic unit cell parameters of lead tartrate crystals are: a = 7.99482 Å, b = 8.84525 Å, c = 8.35318 Å with space group $P2_12_12_1$ [22], while the orthorhombic unit cell parameters of cobalt tartrate crystals are: a = 9.9873 Å, b = 7.8973 Å, c = 10.9832 Å with space group $P2_12_12$ [5]. It is observed that when cobalt is added into the lead levo tartrate, the intensity of all the peaks of mixed crystals of Pb and Co is reduced. The scattering intensities for X-rays are directly related to the number of electrons in the atom. Hence, light atoms scatter X-rays weakly, while heavy atoms scatter X-rays more effectively. Therefore, doping of light element, i.e., Co, reduces the intensity of peaks. The percentage weight of cobalt in the structure of mixed cobalt-lead levo tartrate crystals grown at gel-liquid interface of samples (I-IV) is very less and, therefore, the unit cell parameters of mixed crystals are close to the unit cell parameters of pure lead levo tartrate. In the case of crystals grown below gel-liquid interface of sample (I), the percentage weight of cobalt is high compared to lead and, therefore, the unit cell parameters are altered and attempt to approach to the unit cell parameters of cobalt tartrate. It is also observed that the most intense peaks of pure lead tartrate (020) at 21.12°, (022) at 29.44°, (031) at 32.25°, (131) at 34.17°, (311) at 36.25°, (040) at 40.88°, (033) at 44.71°, and (261) at 68.79° are shifted very little from their position in the sample (I-IV). This indicates that there is no strain produced in the structure of pure lead tartrate due to doping of cobalt because of low ionic radius of cobalt (0.65 Å) compared to lead (1.19 Å) [23]. The peaks of Pb and Co are separately identified in the mixed crystals of lead and cobalt levo tartrate grown below the gel-liquid interface of sample (I). The main peaks in powder XRD pattern of the spherulitic crystals of sample (I) as (200)

DOI: 10.15680/IJIRSET.2014.0310016

ISSN: 2319-8753

International Journal of Innovative Research in Science, Engineering and Technology

(An ISO 3297: 2007 Certified Organization)

Vol. 3, Issue 9, September 2014

at16.86°, (300) at 25.31°, (302) at 32.63°, (032) at 39.11°, (141) at 46.77°, (600) at 51.77°, (334) at 59.91° and (060) at 69.59° can be assigned to cobalt tartrate phase [5]. Similarly, the main peaks of powder XRD patterns of pure lead tartrate indicated above, which are found in the spherulitic crystals of sample (I) as (020) at 21.81°, (311) at 29.44°, (302) at 32.63°, (320) at 33.58°, (401) at 35.48°, (032) at 39.11°, (040) at 44.52° and (253) at 68.18° with variations. This is indicating the presence of cobalt in higher proportion in the grown crystals, probably with separate phase. While the peaks of cobalt tartrate are not separately identified for the crystals grown at the gel-liquid interface of samples (I-IV), indicating less amount of cobalt in the grown crystals and probably substitution of cobalt for lead in the crystals. From table 2, one can find that all the samples (I-IV) exhibit orthorhombic structure. This is indicates that the same nature of lead tartrate persists in the mixed crystals of lead and cobalt levo tartrate grown at the gel-liquid interface of samples (I-IV) with low cobalt concentration, however, the nature changes for the spherulitic crystals of sample (I) with higher cobalt concentration.

Table 2. Unit cell parameters and system for samples (I-IV)

Sample Name	Unit cell parameters	System
Sample I at gel-liquid interface	a = 7.9940 Å , b = 8.8350 Å , c = 8.3530 Å	Orthorhombic α = β = γ = 90°
Sample II at gel-liquid interface	a = 7.9920Å, b = 8.8380 Å, c = 8.3520 Å	Orthorhombic α = β = γ = 90°
Sample III at gel-liquid interface	a = 7.9910 Å, b = 8.8395 Å, c = 8.3510 Å	Orthorhombic α = β = γ = 90°
Sample IV at gel-liquid interface	a = 7.9905 Å, b = 8.8395 Å, c = 8.3510 Å	Orthorhombic α = β = γ = 90°
Sample I below gel-liquid interface	a = 10.58 Å, b = 8.105 Å, c = 8.90 Å	Orthorhombic α = β = γ = 90°

FTIR Study

The FTIR spectra are shown in figure 3.

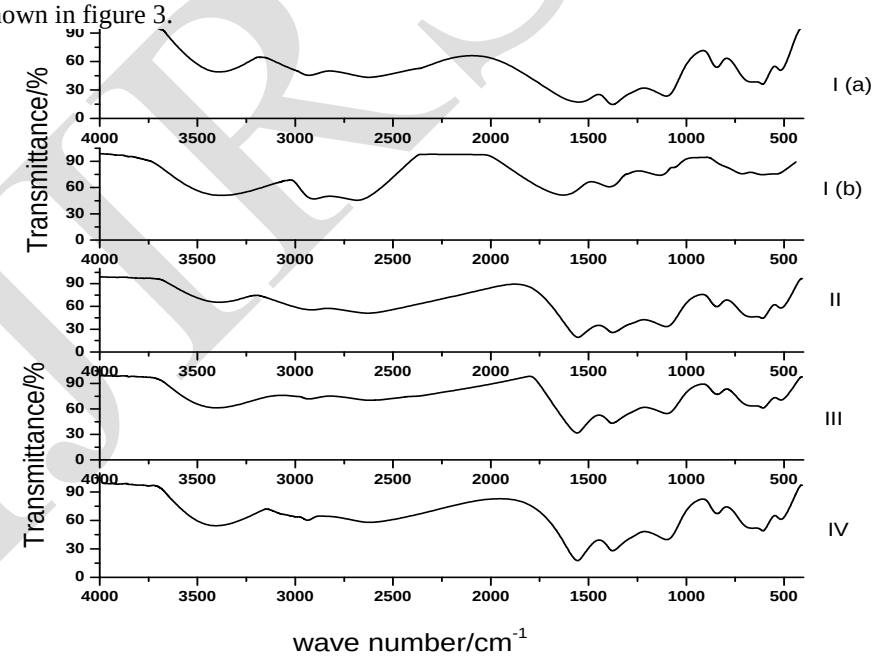

Fig. 3. FTIR spectra of samples (I-IV)

DOI: 10.15680/IJIRSET.2014.0310016

ISSN: 2319-8753

International Journal of Innovative Research in Science, Engineering and Technology

(An ISO 3297: 2007 Certified Organization)

Vol. 3, Issue 9, September 2014

The plots I(a), II, III and IV are for the dendrite crystals near the gel-liquid interface and the plot I(b) is for the spherulitic crystals below gel interface for sample I. The observed vibrational frequencies and their assignments are listed in the table 3. It can be observed from the spectra that the band between 3425 cm^{-1} to 3440 cm^{-1} is due to free O-H stretching vibrations representing water of crystallization or moisture on the surface. The absorption taking place around 2633 cm^{-1} is due to bonded O-H stretching. The absorptions occurring nearly 2930 cm^{-1} and 1385 cm^{-1} are due to asymmetrical C-H stretching and C-H bending of alkane, respectively. The bands observed at 1572 cm^{-1} and 1604 cm^{-1} are due to C=O stretching. The absorptions within 1075 cm^{-1} to 1130 cm^{-1} are due to C-O stretching vibrations. The absorptions occurring between 695 cm^{-1} to 870 cm^{-1} are due to C-C bending vibrations. The absorption bands found between 510 cm^{-1} to 630 $cm^{-1}$are due to the metal-oxygen bonding vibration. Sheveheko [24] studied the IR spectra of some metal tartrate compounds and proposed the formula as follows.

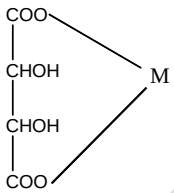

Also, Kirschner and Kiesling [24] studied Cu(II) tartrate by IR spectroscopy and concluded that tartrate was coordinated to Cu(II) through hydroxyl and 2-carboxylate groups.

Table 3. FTIR spectral data for samples (I-IV) for gel interface crystals

Assignments	Wave number/cm^{-1} Sample (Ia) at gel interface	Wave number/cm^{-1} Sample (Ib) below gel interface	Wave number/cm^{-1} Sample (II) at gel interface	Wave number/cm^{-1} Sample (III) at gel interface	Wave number/cm^{-1} Sample (IV) at gel interface
Free O-H Stretching	3426.84	3440.61	3426.04	3435.69	3437.91
C-H Stretching (asymmetrical)	2935.53	2935.00	2936.86	2936.23	2937.33
Bonded O-H Stretching	2633.68	2633.00	2633.93	2634.74	2634.07
C=O Stretching	1572.98	1604.60	1573.10	1573.00	1572.82
C-HBanding (Alkane)	1383.89	1384.79	1383.79	1383.93	1383.83
C-O Stretching	1128.23	1116.78	1128.72	1076.20	1097.17
C-C Bending	867.09, 696.98	716.33	867.12, 696.98	836.35	844.98
Pb-O and Co-O Stretching	605.52, 514.49	615.93, 507.96	605.83, 514.84	621.13, 514.41	628.64, 565.61

It can be seen from the table 3 that the composition of cobalt and lead in the mixed tartrate crystals does not have major effect on various absorptions in FTIR spectra. In the pure lead tartrate crystal, the absorption corresponding to O-H stretching vibration occurs at 3384.9 cm^{-1} [8], while in the pure cobalt tartrate crystal, the strong and sharp absorption corresponding to O-H stretching vibration occurs between 3640 cm^{-1} to 3610 cm^{-1} [4]. As cobalt is doped into lead, this vibration occurs between 3425 cm^{-1} to 3440 cm^{-1}, i.e., the shifts is towards cobalt. This is also indicates the presence of cobalt into the structure. Moreover, in metal tartrate compounds, the metal coordinates with hydroxyl and carboxylates groups; the change in O-H stretching vibration due to presence of cobalt in lead tartrate is thus confirmed. Metal-oxygen vibrations for pure lead tartrate occur between 513.8 cm^{-1} to 605.4 cm^{-1} [7], while the same for cobalt tartrate occur below 500 cm^{-1} [5]. As shown in the table 1, the metal-oxygen vibrations for the mixed crystals of lead and cobalt occur between 505 cm^{-1} to 630 cm^{-1}, indicating no significant effect of cobalt on the metal-oxygen vibrations. This may be because of the low weight percentage of cobalt in the structure. There is no significant effect of cobalt on other absorptions in FTIR spectra.

DOI: 10.15680/IJIRSET.2014.0310016

ISSN: 2319-8753

International Journal of Innovative Research in Science, Engineering and Technology

(An ISO 3297: 2007 Certified Organization)

Vol. 3, Issue 9, September 2014

Thermal behavior

There are reports available in literature on thermal studies on metal tartrate systems, for example, cobalt tartrate [4], ternary iron-manganese-cobalt tartrate compound [9] and ternary iron-manganese-nickel tartrate compound [10]. Figure 4 and 5 show the thermo-gram for the crystals near the gel-liquid interface and below the gel interface of sample (I-IV), respectively.

For the crystals grown at gel-liquid interface of sample (I-IV) and below gel-liquid interface of sample (II-IV), the first stage of dehydration is completed up to temperature 220^{o}C, which results into formation of anhydrous lead-cobalt mixed tartrate. The second stage of decomposition for the same samples is completed up to temperature 290^{o}C by converting the anhydrous sample into carbonate from. In figure 4, the samples (I), (II) and (IV) indicate more stable carbonate stage in comparison to sample (III). During the third and final stage of decomposition up to temperature 400^{o}C, the sample is converted into oxide form.

In case of thermo-gram of the crystals grown below the gel-liquid interface for sample (I), the first stage of dehydration occurs between 50 – 150^{o}C, resulting into formation of anhydrous lead-cobalt mixed tartrate. During the second stage between 150 – 350^{o}C, the anhydrous sample is converted into metastable carbonate form. The final stage of decomposition occurring between 350 – 380^{o}C, converts the sample into oxide form.

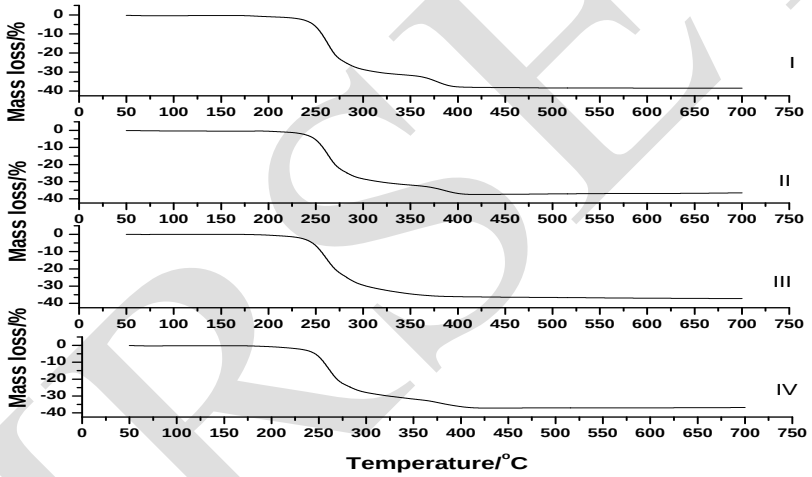

Fig. 4. TG curves of sample (I-IV) grown at gel-liquid interface

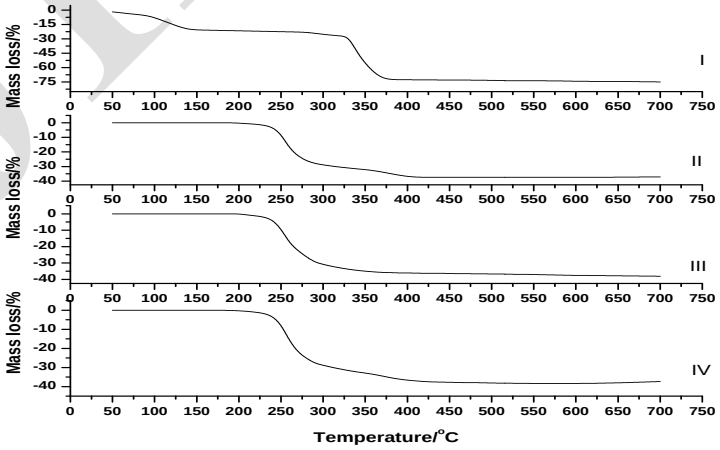

Fig. 5. TG curves of sample (I-IV) grown below gel-liquid interface

DOI: 10.15680/IJIRSET.2014.0310016

ISSN: 2319-8753

International Journal of Innovative Research in Science, Engineering and Technology

(An ISO 3297: 2007 Certified Organization)

Vol. 3, Issue 9, September 2014

Table 4. Theoretical and experimental mass loss values of samples (I-IV) for the dendrite crystals grown at gel-liquid interface

Sample name	Temperature/ (°C)	Reactions involved	Theoretical mass loss/ %/ calculated	Experimental mass loss/ %/ from graph
Sample I	50 – 175°C	No decomposition	100	100
	175 – 190°C	$Pb_{98.68}Co_{1.32}C_4H_4O_6{\cdot}0.15H_2O \rightarrow Pb_{98.68}Co_{1.32}C_4H_4O_6 + 0.15H_2O$	0.76	0.951
	190 – 280°C	$Pb_{98.68}Co_{1.32}C_4H_4O_6 \rightarrow Pb_{98.68}Co_{1.32}CO_3 + CH_4 + 2CO + ½\ O_2$	25.50	24.76
	280 – 400°C	$Pb_{98.68}Co_{1.32}CO_3 \rightarrow Pb_{98.68}Co_{1.32}O + CO_2$	37.87	37.86
Sample II	50 – 190°C	No decomposition	100	100
	190 – 220°C	$Pb_{99.39}Co_{0.61}C_4H_4O_6{\cdot}0.2H_2O \rightarrow Pb_{99.39}Co_{0.61}C_4H_4O_6 + 0.2H_2O$	1.01	1.08
	220 – 280°C	$Pb_{99.39}Co_{0.61}C_4H_4O_6 \rightarrow Pb_{99.39}Co_{0.61}CO_3 + CH_4 + 2CO + ½\ O_2$	25.60	24.10
	280 – 400°C	$Pb_{99.39}Co_{0.61}CO_3 \rightarrow Pb_{99.39}Co_{0.61}O + CO_2$	37.91	37.04
Sample III	50 – 190°C	No decomposition	100	100
	190 – 220°C	$Pb_{99.66}Co_{0.34}C_4H_4O_6{\cdot}0.2H_2O \rightarrow Pb_{99.66}Co_{0.34}C_4H_4O_6 + 0.2H_2O$	1.01	1.12
	220 – 280°C	$Pb_{99.66}Co_{0.34}C_4H_4O_6 \rightarrow Pb_{99.66}Co_{0.34}CO_3 + CH_4 + 2CO + ½\ O_2$	25.48	24.06
	280 – 400°C	$Pb_{99.66}Co_{0.34}CO_3 \rightarrow Pb_{99.66}Co_{0.34}O + CO_2$	37.78	36.10
Sample IV	50 – 190°C	No decomposition	100	100
	190 – 210°C	$Pb_{99.78}Co_{0.22}C_4H_4O_6{\cdot}0.2H_2O \rightarrow Pb_{99.78}Co_{0.22}C_4H_4O_6 + 0.2H_2O$	1.01	1.16
	210 – 290°C	$Pb_{99.78}Co_{0.22}C_4H_4O_6 \rightarrow Pb_{99.78}Co_{0.22}CO_3 + CH_4 + 2CO + ½\ O_2$	25.57	26.60
	290 – 400°C	$Pb_{99.78}Co_{0.22}CO_3 \rightarrow Pb_{99.78}Co_{0.22}O + CO_2$	37.86	36.36

Table 5. Theoretical and experimental mass loss values of samples (I-IV) for the crystals below gel-liquid interface

Sample name	Temperature/ (°C)	Reactions involved	Theoretical mass loss/ %/ calculated	Experimental mass loss/ %/ from graph
Sample I	0 – 50°C	No decomposition	100	100
	50 – 150°C	$Pb_{45.79}Co_{54.21}\ (C_4H_4O_6)_2\ 6H_2O \rightarrow Pb_{45.79}Co_{54.21}\ (C_4H_4O_6)_2 + 6H_2O$	20.35	20.63
	150 – 340°C	Anhydrous form $Pb_{45.79}Co_{54.21}\ (C_4H_4O_6)_2$ is almost stable	no mass loss	no mass loss
	340 – 380°C	$Pb_{45.79}Co_{54.21}\ (C_4H_4O_6)_2 \rightarrow Pb_{45.79}OCd_{54.21}O + 2CH_4 + 6CO + 2O_2$	70.10	72.32
Sample II	50 – 190°C	No decomposition	100	100
	190 – 220°C	$Pb_{99.33}Co_{0.67}C_4H_4O_6{\cdot}0.2H_2O \rightarrow Pb_{99.33}Co_{0.67}C_4H_4O_6 + 0.2H_2O$	1.01	1.03
	220 – 280°C	$Pb_{99.33}Co_{0.67}C_4H_4O_6 \rightarrow Pb_{99.33}Co_{0.67}CO_3 + CH_4 + 2CO + ½\ O_2$	25.61	26.11

DOI: 10.15680/IJIRSET.2014.0310016

ISSN: 2319-8753

International Journal of Innovative Research in Science, Engineering and Technology

(An ISO 3297: 2007 Certified Organization)

Vol. 3, Issue 9, September 2014

	280 – 400°C	$Pb_{99.33}Co_{0.67}CO_3 \rightarrow Pb_{99.33}Co_{0.67}O + CO_2$	37.92	36.74
Sample III	50 – 190°C	No decomposition	100	100
	190 – 220°C	$Pb_{99.43}Co_{0.57}C_4H_4O_6 \cdot 0.2H_2O \rightarrow Pb_{99.43}Co_{0.57}C_4H_4O_6 + 0.2H_2O$	1.01	1.2
	220 – 280°C	$Pb_{99.43}Co_{0.57}C_4H_4O_6 \rightarrow Pb_{99.43}Co_{0.57}CO_3 + CH_4 + 2CO + ½ O_2$	25.48	26.20
	280 – 400°C	$Pb_{99.43}Co_{0.57}CO_3 \rightarrow Pb_{99.43}Co_{0.57}O + CO_2$	37.91	36.12
Sample IV	50 – 190°C	No decomposition	100	100
	190 – 210°C	$Pb_{99.76}Co_{0.24}C_4H_4O_6 \cdot 0.2H_2O \rightarrow Pb_{99.76}Co_{0.24}C_4H_4O_6 + 0.2H_2O$	1.01	1.08
	210 – 290°C	$Pb_{99.76}Co_{0.24}C_4H_4O_6 \rightarrow Pb_{99.76}Co_{0.24}CO_3 + CH_4 + 2CO + ½ O_2$	25.57	25.22
	290 – 400°C	$Pb_{99.76}Co_{0.24}CO_3 \rightarrow Pb_{99.76}Co_{0.24}O + CO_2$	37.86	36.63

Table 4 and 5 give details of the thermal decomposition of the samples (I-IV) for the crystals grown at gel-liquid interface and below gel-liquid interface with theoretically calculated and experimentally obtained mass loss values, respectively. The subscript values are in percentage. The amount of water molecules attached with samples (I-IV) for the crystals at gel-liquid interface and for the crystals below the gel-liquid interface have been calculated and given in table 6 with stoichiometric formula. From figure 4 and 5, one can notice that the decomposition of dehydrated samples starts within the range of 190°C to 220°C except for the sample (I) in figure 5, where it starts around 350°C. This is due to higher concentration of cobalt in the samples. In pure cobalt tartrate, the anhydrous cobalt tartrate starts decomposition around 340°C [4]. Also, no carbonate stage is observed. Anhydrous form of cobalt lead tartrate of sample (I) obtained from the bottom of test tube are more stable than other samples and possess more water of hydration than other samples. All other samples possess less than one water molecule associated with, which may be due to moisture content.

Table 6. Stoichiometric formula for the Pb Co mixed levo tartrate crystals

Sample No.	Proposed formula	Estimated formula from EDAX and TGA	
		crystals near the gel-liquid interface	crystals below the gel-liquid interface
I.	$Pb_{0.2}Co_{0.8}C_4H_4O_6 \cdot nH_2O$	$Pb_{98.68}Co_{1.32}C_4H_4O_6 \cdot 0.15H_2O$	$Pb_{45.79}Co_{54.21}C_4H_4O_6 \cdot 6H_2O$
II.	$Pb_{0.4}Co_{0.6}C_4H_4O_6 \cdot nH_2O$	$Pb_{99.39}Co_{0.61}C_4H_4O_6 \cdot 0.2H_2O$	$Pb_{99.33}Co_{0.67}C_4H_4O_6 \cdot 0.2H_2O$
III.	$Pb_{0.6}Co_{0.4}C_4H_4O_6 \cdot nH_2O$	$Pb_{99.66}Co_{0.34}C_4H_4O_6 \cdot 0.2H_2O$	$Pb_{99.43}Co_{0.57}C_4H_4O_6 \cdot 0.2H_2O$
IV.	$Pb_{0.8}Co_{0.2}C_4H_4O_6 \cdot nH_2O$	$Pb_{99.78}Co_{0.22}C_4H_4O_6 \cdot 0.2H_2O$	$Pb_{99.76}Co_{0.24}C_4H_4O_6 \cdot 0.2H_2O$

V. CONCLUSIONS

The lead-cobalt levo tartrate crystals were grown by single diffusion gel technique in silica hydro gel medium. The dendrite type crystals were grown at gel-liquid interface and spherelutic as well as spiky crystals were grown in the gel column below the gel-liquid interface. It was found that the metallic content did not change in the grown crystals as per the composition of supernatant solution containing lead nitrate and cobalt nitrate. The EDAX analysis for gel-liquid interface grown crystals and below the gel-liquid interface grown crystals suggested that cobalt entered into the lattice in less amount with comparision to lead, which is due to the higher hydrated radius of Co^{+2} ions compared to Pb^{+2} ions. The FTIR spectra of the grown crystals indicated the presence of O-H, C-H, C-O, C-C and C=O functional groups with metal-oxygen vibrations. The powder XRD study of the grown crystals at gel-liquid interface suggested the orthorhombic crystal structure and the unit cell parameters were indicating that the nature of parent compound lead tartrate persisted in the mixed lead cobalt levo tartrate crystals with high lead percent values. From the thermo-grams it was found that the crystals grown at gel-liquid interface and below gel-liquid interface were thermally unstable. On heating they became anhydrous and decomposed into metal oxides through a single stage of carbonate. While the spherulitic crystals grown below the gel-liquid interface having higher cobalt in their structure compared to lead,

ISSN: 2319-8753

International Journal of Innovative Research in Science, Engineering and Technology

(An ISO 3297: 2007 Certified Organization)

Vol. 3, Issue 9, September 2014

exhibited different behavior. The presence of water molecules was detected and calculated. The exact stoichiometric formulations for mixed crystals were suggested.

ACKNOWLEDGMENTS

The author (Harshkant Jethva) is working as an associate professor in Physics at Maharaja Shree Mahendrasinhji Science College, Morbi, Gujarat and doing research under the guidance of Prof. Mihir Joshi, Department of Physics, Saurashtra University, Rajkot, Gujarat. The authors are thankful to Prof. H.H. Joshi (HOD, Physics) for his keen interest and the author (Harshkant Jethva) is thankful to the Principal and the Management of Maharaja Shree Mahendrasinhji Science College, Morbi for encouragements.

REFERENCES

[1] S. J. Shitole, K B Saraf, Growth and study of some gel grown group II single crystals of iodate, Bull. Mater. Sci. 5 (2001) 461.
[2] S. L. Garud, K. B. Saraf, Growth and study of mixed crystals of Ca-Cd iodate, Bull. Mater. Sci. 4 (2008) 639.
[3] S. Joseph, H. S. Joshi, M. J. Joshi, Infrared spectroscopic and thermal studies of gel grown spherulitic crystals of iron tartrate, Cryst. Res. Technol. 32(2) (1997) 339.
[4] S. J. Nandre, S. J. Shitole, R. R. Ahire, FT-IR, thermal and optical studies of gel grown cobalt tartrate crystals, J. Nano Electron. Phys. 5 (2013) 04050.
[5] V. Mathivanan, M. Haris, T. Prasanyaa, M. Amgalan, Synthesis and characterization of gel-grown cobalt tartrate crystals, Pramana J. Phys. 82(3) (2014) 537.
[6] S. Ariponnammal, T. Srinivasan, Growth and spectroscopic characterization of cobalt tartrate crystals, Res. J. Recent. Sci. 3 (2014) 63.
[7] H. O. Jethva, M. V. Parsania, Growth and characterization of lead tartrate crystals, Asian J. Chem. 22(8) (2010) 6317.
[8] S. J. Joshi, B. B. Parekh, K. D. Parikh, K. D. Vora, M. J. Joshi, Growth and characterization of gel grown pure and mixed iron-manganese levo-tartrate crystals, Bull. Mater. Sci. 29(3) (2006) 307.
[9] S. J. Joshi, K. P. Tank, B. B. Parekh, M. J. Joshi, Characterization of gel grown iron-manganese-cobalt ternary levo-tartrate crystals, Cryst. Res. Technol. 45 (2010) 303.
[10] S. J. Joshi, K. P. Tank, B. B. Parekh, M. J. Joshi, FT-IR and thermal studies of iron-nickel-manganese ternary levo-tartrate crystals, J. Therm. Anal. Calorim. (2012) doi:10.1007/s10973-012-2624-8.
[11] I. G. Casella, J. Electroanal. Chem. 520(1-2), 119 (2002)
[12] N. J. Rahway, The Merck index of chemicals and drugs, 6th ed, Merck and Co. 1952.
[13] H. K. Henisch, Crystal Growth in Gels, Dover Publication, New York, 1993.
[14] K. Fujiwara, K. Nakajima, Mechanism of dendritic crystal growth, Springer, 2009.
[15] M. Abdulkadhar, M. A. Ittyachen, Development of lead tartrate crystals from its dendritic form, J. Cryst. Growth. 39 (1977) 365.
[16] R. M. Dabhi, B. B. Parekh, M. J. Joshi, Dielectric studies of gel grown zinc tartrate crystals, Indian J. Phys. 79(5) (2005) 503.
[17] A. D. Saraf, K. B. Saraf, P. A. Wani, S. V. Bhoraskar, Dendritic growth of ammonium tartrate single crystals in silica gel, Cryst. Res. Technol. 21(4) (1986) 449.
[18] P. N. Kotru, N. K. Gupta, K. K. Raina, Growth of lanthanum tartrate crystals in silica gel, J. Mater. Sci. 21 (1986) 90.
[19] S. Joseph, Ph. D. Thesis Saurashtra University Rajkot India, 1997.
[20] Dove, Nix, Ionic hydration in chemistry and biophysics, Geochim. Cosmochim. Acta. 61 (1997) 3331.
[21] C. F. Albert, G. Wilkinson, P. L. Gaus, Basic Inorganic Chemistry, 3rd ed. John Wiley and Sons, 1995.
[22] D. J. A. De Ridder, K. Goubitz, E. J. Sonneveld, W. Molleman, H. Schenk, Lead tartrate from x-ray powder diffraction data, Cryst. Stru. Comm. C58 (2002) m596.
[23] B. D. Cullity, Elements of x-ray diffraction, Addison-Wesley Publishing Company. 1978.
[24] S. J. Joshi; *Ph. D. Thesis*, Saurashtra University, Rajkot (2009).